Journal of Science and Transport Technology
Journal homepage: https://jstt.vn/index.php/en

Effect of shearing rate and cyclic load on shear strength of coral sand

Duc Tiep Pham[1], Van Tuan Vu[1*], Thi Lua Hoang[2], Duc Phong Pham[1], Nam Hung Tran[1], Duc Dung Phi[1], Vu Dinh Tho[3], Tuan Anh Pham[3]
[1]Institute of Construction Technology, Le Quy Don Technical University, Hanoi 100000, Vietnam
[2]Faculty of Civil Engineering, Thuy loi University, Hanoi 100000, Vietnam
[3]Smart Urban Construction Infrastructure, University of Transport Technology, Hanoi 100000, Vietnam

Article info
Type of article:
Original research paper

DOI:
https://doi.org/10.58845/jstt.utt.2026.en.6.2.409-428

[*]**Corresponding author:**
Email address:
vantuanvu@lqdtu.edu.vn

Received: 08/11/2025
Received in Revised Form: 22/04/2026
Accepted: 06/05/2026

Abstract: Coral sand is characterized by non-uniform gradation, angular and elongated particle shapes, and a hollow, fragile structure. Although the shear strength behavior of coral sand has been investigated in previous studies, the effects of shear rate and repeated shear displacement on its shear behavior have not yet been fully clarified. This study investigates the shear behavior of coral sand using direct shear tests conducted under saturated conditions, in which the effects of shear rate and repeated displacement are evaluated independently. A total of 74 direct shear tests were performed on coral sand specimens prepared at two relative densities (D_r). To investigate the effect of shear rate, tests were carried out under three normal stresses (σ = 50, 100, and 200 kPa) and nine shear rates ranging from 0.01 to 5 mm/min. In a separate test series, quasi-static cyclic displacement-controlled direct shear tests were conducted on medium-dense and dense specimens to examine the influence of repeated shear displacement. In these tests, each cycle corresponds to one complete forward and backward shear displacement with a prescribed amplitude. Five displacement cycle levels (10, 20, 30, 40, and 45 cycles) with different displacement amplitudes were considered. The experimental results show that a characteristic shear rate (SR_{so}), corresponding to the minimum measured shear force, can be identified for each relative density in the shear-rate-controlled tests. The variation of internal friction angle with shear rate generally follows the trend of shear force, whereas the apparent cohesion at D_r = 75% exhibits a different tendency. In the quasi-static cyclic displacement tests, medium-dense coral sand tends to exhibit a larger increase in peak shear force than dense coral sand. These observations provide experimental insight into the shear behavior of coral sand under loading conditions relevant to coastal and island engineering applications.
Keywords: shearing rate; shear force; shear strength; cyclic load; coral sand.

1. Introduction

Tropical oceans contain extensive coral reefs, coral reefs after their life span's end turn into coral sands due to the impact of the environment. Coral sand is primarily formed by calcium carbonate and fragments of coral reefs. The specifications of coral sand as a material include non-uniform gradation and a variety of angular and

elongated particle shapes. Additionally, coral sand particles have a hollow and fragile structure [1]. Throughout time, coral islands and embankments made of coral sand, which surround coastal lands in coral areas, have formed. Because of the unique properties of coral sand, it is necessary to understand the behavior of coral sand when designing and constructing structures on the coral sand ground.

Shear strength is the principal engineering property of soil, which controls the stability of structures under structural loads. Shear strength parameters are essential for determining bearing capacity, designing retaining walls, assessing slope and embankment stability, and various other applications. Currently, to investigate soil shear strength characteristics, triaxial compression and direct shear tests are usually employed [2, 3, 4, 5, 6, 7]. For coral sand, some studies have been conducted to determine shear strength parameters of the sand, considering the influence of several aspects. WEN et al [8] noted that the internal friction angle of coral sand is influenced not only by compactness but also by water content. They discovered that lower water content and higher compactness result in greater shear properties. Wang et al [9] presented a fundamental calculation of coral sand's shear strengths, considering the impact of compactness and values of vertical load. The findings demonstrated that shear strength increased with both the increase in vertical load and compactness. The relationship between particle size distribution and shear strength of coral sands was investigated by Zhang et al [10]. This study revealed variations in the deviatoric stress-strain curve among specimens with different grain distributions. Changes in the internal friction angle were observed in a parabolic manner with alterations in fine particle content, and cohesion decreased as the non-uniformity in particle sizes was increased.

The coral embankment often suffers offshore environmental loads transferred from the upper structure to the embankment. Offshore environmental loads usually exhibit two distinctive characteristics: a significant magnitude of lateral load and cyclic loading. These two characteristics of offshore environmental loads are related to the shear rate, the number of cycles, and the amplitude of cyclic loads. Through the experiments, some previous studies have reported the significant impact of shear rate and strain rate on the shear strength behaviors. Beren et al [11] discovered that both the internal friction angle and peak shear strength values increased with increasing shear rate. In a study by Yamamuro et al.[12], the effect of strain rate on stress-strain behavior was investigated using triaxial tests. The experiment involved specimens with compactness levels of 30% and 60%, vacuum-confined axisymmetric specimens, and two different confining pressures (98 and 350 kPa). The results indicated a noticeable increase in elastoplastic stiffness with an increase in strain rate. Sweta and Hussaini [13] examined the effect of shearing rate on the behavior of geogrid-reinforced railroad ballast under direct shear conditions. The conclusion drawn was that an increase in shearing rate led to a decrease in the internal friction angle of ballasts.

Impact of cyclic loading conditions on the shear strength properties of sand has been conducted in several studies. Research by Silver et al [14] on silica sand demonstrated that an increase in the number of cycles led to a reduction in effective vertical stress and effective horizontal stress. Similar conclusions were drawn from the studies by Erken and Ulker [15], Doan et al. [16], and Ray et al. [17]. These studies consistently indicated a downward trend in cyclic shear stress with an increase in the number of cycles in experiments. For coral sand, Ding et al. [18], He et al. [19], Wang and Zha [20], and Ma et al. [21] carried out monotonic and cyclic triaxial tests, whereas You et al. [22] employed a cyclic hollow-cylinder shear apparatus for fixed-axis shear tests. The findings highlight the unique shear behavior,

compressibility, and particle breakage characteristics of coral sand in contrast to siliceous sand.

From the literature survey, it can be affirmed that cyclic load conditions can affect the shear strength characteristics of soil. However, there is a scarcity of studies that consider the shear characteristics of coral sand in relation to shear rate and cyclic load. Since coral embankments are often subjected to special loads with characteristics such as repetition, changes in magnitudes, and shear rates, it is necessary to study the impact of these load properties on the shear strength characteristic of coral sand. In this study, the shear strength behaviour of coral sand will be investigated through both direct shear tests and cyclic shear tests, considering the above special load characteristics. Two sets of test samples with varying compactness levels (medium dense D_r=50% and dense D_r=75%) were experimented upon. Three levels of normal stresses (σ=50kPa, σ=100kPa, σ=200kPa) and nine shear rates (SR=0.01mm/min to 5mm/min) will be applied. Cyclic shear tests are conducted at two levels of cyclic horizontal displacement (0.8mm and 1.6mm) under five different cycle types (10 cycles, 20 cycles, 30 cycles, 40 cycles, 45 cycles). After completing the specified number of cycles, shear tests were conducted until the sample sustained damage, allowing the determination of the peak shear force. The following sections will present in detail about studied sand, methodology, results, and discussions.

2. Material characteristics

The coral sand used in this study was collected from an offshore island in Viet Nam's East Sea. Field sampling was carried out from an embankment fill constructed in a coastal environment, where the water level varies periodically due to tidal action. Under such conditions, the application of conventional compaction control methods prescribed in current Vietnamese standards is difficult, and the achieved field compactness is typically non-uniform and uncertain. In practice, densification of the embankment is not governed by controlled mechanical compaction, but rather by a combination of repeated traffic loading, self-weight rearrangement of particles, and cyclic wetting–drying associated with tidal water-level fluctuations. These mechanisms contribute to soil densification mainly in a qualitative sense, and their effects are difficult to quantify using standard in situ testing methods. Therefore, to obtain a quantitative and representative estimate of the compactness of the embankment material, an open excavation method combined with tube sampling was adopted, and the sampling was conducted during periods of low tide. This timing allowed the excavation and tube insertion to be performed under relatively stable and accessible conditions, while minimizing disturbance caused by water inflow and facilitating a more reliable assessment of the in situ compactness. The open excavation procedure involved digging a pit with a width, length, and depth of approximately 1 m. A cylindrical tube with a diameter of 13 cm and a height of 45 cm was then placed vertically at the bottom of the pit and driven into the sand using a wooden plate and a hammer. The surrounding sand was carefully removed, and the tube was extracted and sealed to minimize moisture loss. Photographs illustrating the sampling procedure are presented in Fig. 1.

It should be emphasized that the material obtained from the field was not used directly as undisturbed specimens for shear testing. Field sampling was performed to characterize the material properties, including grain-size distribution and an indicative range of in situ compactness. All specimens used in the direct shear tests were reconstituted samples. Loose coral sand (or silica sand used for comparison) was placed into the shear box and compacted in layers to achieve the prescribed relative densities of D_r = 50% and 75%. The compactness inferred from field sampling was

used only as a reference for selecting these target Dr values, and not as an indication that undisturbed samples were tested.

The particle-size distribution curve of the coral sand is shown in Fig. 2. Furthermore, the grain size distribution of the filling sand (silica sand) in the Sao Mai residential area, Binh Khanh 3 ward, Long Xuyen city, An Giang province [23] is also shown in Fig. 2 as a reference material for comparison, representing a commonly used granular fill in engineering practice in Viet Nam. The coral sand exhibits a gentler gradation curve than the fill sand. The main grain size of the fill sand lies in the range of 0.25–0.5 mm, whereas that of the coral sand is more broadly distributed between 0.25 and 1.0 mm. Based on the gradation curve, the uniformity coefficient and curvature coefficient of the coral sand are determined as C_u = 6.31 and C_c = 1.63, respectively. According to ASTM D2487-11 [24], the coral sand is classified as SW (clean, well-graded sand). The physical properties of the studied coral sand are summarized in Table 1.

Fig. 1. Progress of using the open excavation method to take coral sand samples and evaluate the compactness

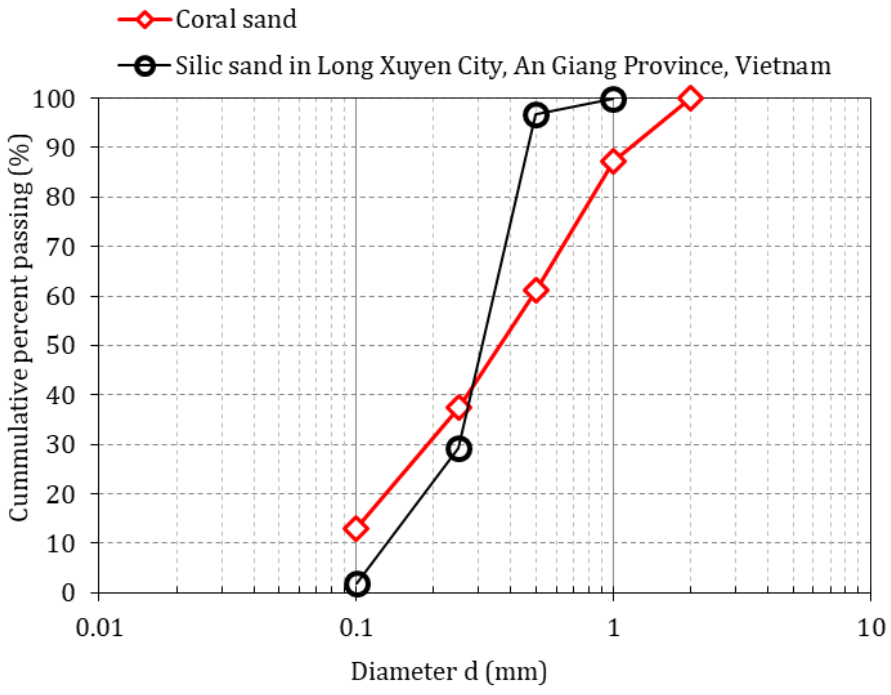

Fig. 2. Particle-size distribution curve of coral sand and silica sand

Table 1. Physical properties of coral sand

Parameter	Value
Density of soil particles, ρ_s (g/cm^3)	2.671
Maximum void ratio, e_{max}	0.927
Minimum void ratio, e_{min}	0.600
Coefficient of uniformity, C_u	6.31
Coefficient of curvature, C_c	1.11

3. Test apparatus and testing programme

All tests were conducted in the Geotechnical Engineering Laboratory of Le Quy Don Technical University, Vietnam. An advanced automated direct shear testing apparatus (SHEARMATIC EmS) was used to perform both monotonic direct shear tests and cyclic shear tests. The apparatus is based on the conventional direct shear device described by Taylor [25] and Skempton and Bishop [26], consisting of an upper and a lower shear box (Fig. 3). During testing, shear is induced along the predefined horizontal interface by pushing the lower shear box horizontally, while a constant vertical load is applied to the upper shear box.

Fig. 4 presents an overview of the experimental setup, including the direct shear box (DSB) and the data acquisition system. According to the SHEARMATIC EmS Manual, accurate axial transmission of horizontal force is ensured through a straight mechanical alignment between the shear box, drive shaft, and load cell. The system is fully automated and controlled via a digital controller operating under Proportional–Integral–Derivative (PID) control, which continuously records and regulates forces and displacements in both vertical and horizontal directions.

The dimensions of the direct shear box were selected in accordance with ASTM D3080 [27] and relevant recommendations [28, 29], based on the maximum particle size of the tested soil. The width of the shear box was chosen to be at least ten times the maximum particle size, and the initial specimen thickness was at least six times the maximum particle size. In this study, specimens were prepared in a cylindrical shape with a diameter D = 63.5 mm and a height H = 20 mm, corresponding to approximately twenty times the maximum particle size of the coral sand.

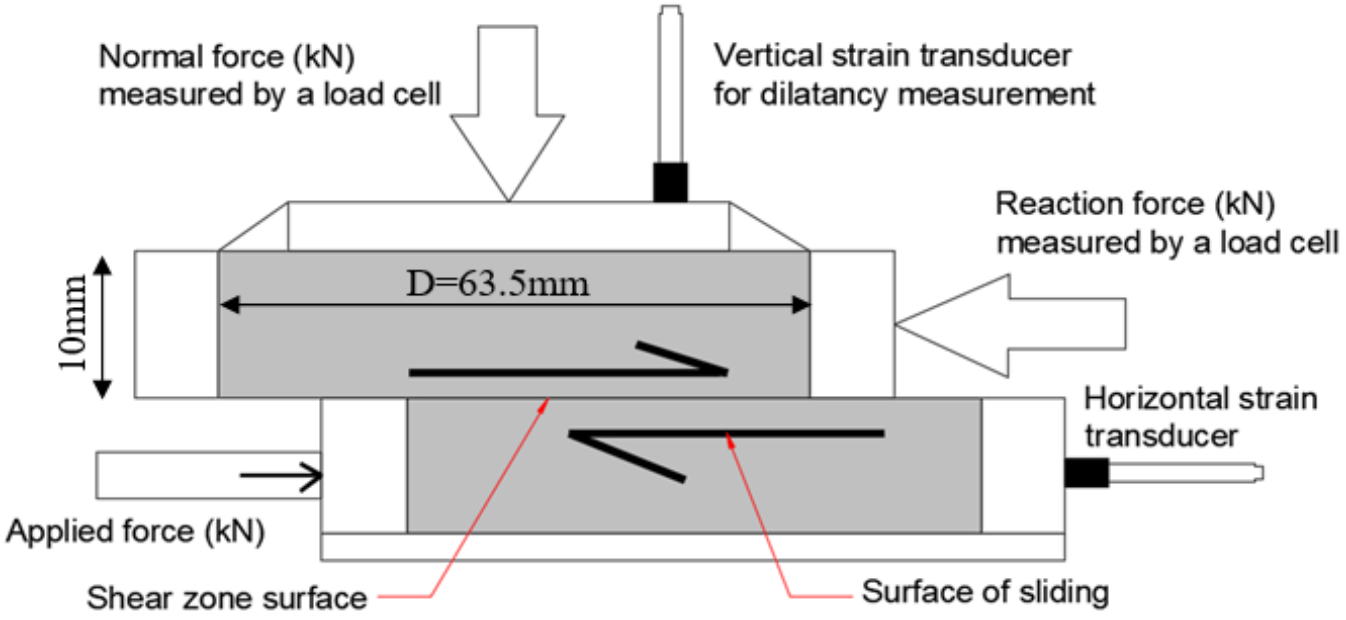

Fig. 3. Scheme of direct shear apparatus

Fig. 4. View of experimental device

All tests were performed under consolidated drained (CD) conditions. After specimen preparation, water was added to fully saturate the sample, reproducing the field condition during high tide. Consolidation was then carried out under vertical loading prior to shearing. To reach the target normal stresses (σ = 50, 100, and 200 kPa), the vertical load was applied incrementally. The initial load level was 25 kPa, and each subsequent load was twice the previous level, with each load increment maintained for 30 minutes to allow consolidation and dissipation of excess pore water pressure. Shearing was initiated only after completion of this consolidation process.

Two levels of specimen compactness were considered: medium-dense (D_r = 50%) and dense (D_r = 75%), selected to represent the range of compactness inferred from field conditions. For each compactness level, monotonic direct shear tests were conducted under three normal stresses (σ = 50, 100, and 200 kPa) and nine shear rates (SR = 0.01, 0.05, 0.1, 0.3, 0.7, 1, 2, 4, and 5 mm/min) to investigate the influence of shear rate on shear strength behavior.

In addition, a series of quasi-static cyclic displacement-controlled shear tests was performed to examine the influence of repeated horizontal shear displacement on the shear strength of coral sand. These tests were conducted on medium-dense (D_r = 50%) and dense (D_r = 75%) specimens using the same shear apparatus. For medium-dense specimens, a shear rate of 0.3 mm/min was applied in both forward and backward directions, whereas dense specimens were tested at a shear rate of 1.0 mm/min in both directions.

In the cyclic shear tests, one cycle corresponds to one complete forward and backward horizontal shear displacement with a prescribed amplitude. Two displacement amplitudes were considered: 0.8 mm and 1.6 mm, corresponding to approximately 20–40% and 29–58% of the displacement at peak shear force for D_r = 50% and D_r = 75%, respectively. Five levels of displacement repetition were examined: 10, 20, 30, 40, and 45 cycles. It should be emphasized that these tests represent low-rate, quasi-static cyclic displacement tests, dominated by particle rearrangement effects, and do not involve dynamic loading or loading frequency.

After completing the prescribed number of displacement cycles, monotonic direct shear loading was applied until failure to determine the peak shear force. The main stages of the experimental programme are illustrated in Figs. 5 to 8.

It is noticed that, a total of 74 testing cases

were conducted. Due to the large number of tests, each test under each condition was performed only once without repetition. Therefore, all the tests were performed carefully following the same preparation protocol and boundary conditions to minimize experimental variability.

Fig. 5. Weighing the coral sand for sample preparation

Fig. 6. Compacting the coral sand within the shear box

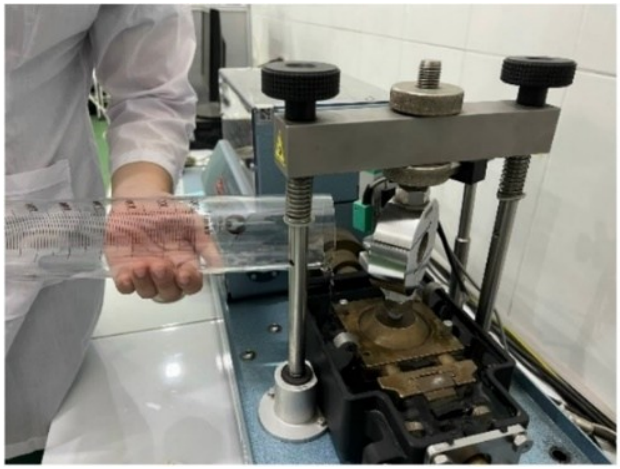

Fig. 7. Saturating the coral sand sample by introducing water into the shear box

Fig. 8. Coral sand sample after completion of a shear test

4. Experimental Results and Discussion

4.1. Effect of Shear Rate on the shear characteristics of coral sand

The peak shear forces obtained from 54 tests under two different relative densities, three levels of normal loads, and nine shear rates are shown in Table 2 and Figs. 9-11. The experimental results show that there was a specific shear rate (SR_{so}) at which the shear force reached its minimum value. For medium-dense samples, the SRso was approximately 0.3mm/min, while for coral sand samples in a dense state, the SR_{so} was around 1.0mm/min.

When the shear rate is below SR_{so}, the increase in shear force with decreasing shear rate can be attributed to more complete drainage resulting from the longer duration of shearing. The longer drainage time allows a larger proportion of excess pore water pressure to dissipate, leading to an increase in effective stress and, consequently, an increase in shear force. By contrast, when the shear rate exceeds SR_{so}, the subsequent increase in shear force may be qualitatively associated with rate-dependent resistance effects arising from the interaction between sand grains and pore water in a saturated granular medium. At higher shear rates, the relative motion between particles and pore water becomes more pronounced, which can introduce an additional resistance component superimposed on the frictional response. In this

context, the concept of viscous resistance often illustrated by Stokes-type drag for a single particle in a viscous fluid [30], is invoked only as a qualitative analogy. Given that the direct shear test involves a dense multi-particle system with complex interactions, no direct quantitative application of Stokes' drag is implied. Accordingly, this discussion is intended to provide a conceptual interpretation of the observed shear-rate dependence at higher shear rates. In addition, the increase in shear force after the shear rate exceeds SRso is less pronounced for the specimen with D_r = 50% than for the specimen with D_r = 75%. This behavior can be attributed to the higher void ratio associated with the lower relative density, which promotes the generation and persistence of excess pore water pressure during shearing [31]. The elevated excess pore water pressure results in a greater reduction in effective stress, thereby limiting the mobilization of interparticle friction and shear resistance. Consequently, the increase in the measured shear force with increasing shear rate is less significant for the medium-dense specimen compared with the dense specimen.

Table 2. Peak shear forces for the coral sand regarding the impact of the shear rate and normal stress at two relative densities

No	Relative density (D_r %)	Dry unit weight (g/cm^3)	Dry mass of specimen (g)	Normal stress (kPa)	Shear rate (mm/min)	Experiment time (min)	Peak shear force (N)
1	50	1.515	91.39	50	0.01	1000.20	213.18
2	50	1.515	91.39	100	0.01	1000.20	382.64
3	50	1.515	91.39	200	0.01	1000.20	652.53
4	50	1.515	91.39	50	0.05	199.80	197.00
5	50	1.515	91.39	100	0.05	199.80	336.33
6	50	1.515	91.39	200	0.05	199.80	591.49
7	50	1.515	91.39	50	0.10	100.20	145.66
8	50	1.515	91.39	100	0.10	100.20	281.14
9	50	1.515	91.39	200	0.10	100.20	576.60
10	50	1.515	91.39	50	0.30	33.60	151.93
11	50	1.515	91.39	100	0.30	33.60	276.38
12	50	1.515	91.39	200	0.30	33.60	547.13
13	50	1.515	91.39	50	0.70	14.40	161.671
14	50	1.515	91.39	100	0.70	14.40	276.81
15	50	1.515	91.39	200	0.70	14.40	604.70
16	50	1.515	91.39	50	1.00	10.20	163.40
17	50	1.515	91.39	100	1.00	10.20	318.15
18	50	1.515	91.39	200	1.00	10.20	590.41
19	50	1.515	91.39	50	2.00	4.80	150.20
20	50	1.515	91.39	100	2.00	4.80	307.98
21	50	1.515	91.39	200	2.00	4.80	593.01
22	50	1.515	91.39	50	4.00	2.40	165.13
23	50	1.515	91.39	100	4.00	2.40	324.21
24	50	1.515	91.39	200	4.00	2.40	621.58
25	50	1.515	91.39	50	5.00	1.80	161.89
26	50	1.515	91.39	100	5.00	1.80	330.92
27	50	1.515	91.39	200	5.00	1.80	627.64
28	75	1.588	95.83	50	0.01	1000.20	242.40
29	75	1.588	95.83	100	0.01	1000.20	381.78
30	75	1.588	95.83	200	0.01	1000.20	689.10
31	75	1.588	95.83	50	0.05	199.80	233.09

Table 2. (continued)

No	Relative density (D_r %)	Dry unit weight (g/cm^3)	Dry mass of specimen (g)	Normal stress (kPa)	Shear rate (mm/min)	Experiment time (min)	Peak shear force (N)
32	75	1.588	95.83	100	0.05	199.80	401.04
33	75	1.588	95.83	200	0.05	199.80	780.00
34	75	1.588	95.83	50	0.10	100.20	227.03
35	75	1.588	95.83	100	0.10	100.20	419.00
36	75	1.588	95.83	200	0.10	100.20	788.44
37	75	1.588	95.83	50	0.30	33.60	232.88
38	75	1.588	95.83	100	0.30	33.60	391.95
39	75	1.588	95.83	200	0.30	33.60	699.28
40	75	1.588	95.83	50	0.70	14.40	223.79
41	75	1.588	95.83	100	0.70	14.40	322.48
42	75	1.588	95.83	200	0.70	14.40	608.38
43	75	1.588	95.83	50	1.00	10.20	209.93
44	75	1.588	95.83	100	1.00	10.20	367.06
45	75	1.588	95.83	200	1.00	10.20	644.74
46	75	1.588	95.83	50	2.00	4.80	222.49
47	75	1.588	95.83	100	2.00	4.80	339.36
48	75	1.588	95.83	200	2.00	4.80	679.58
49	75	1.588	95.83	50	4.00	2.40	221.41
50	75	1.588	95.83	100	4.00	2.40	391.08
51	75	1.588	95.83	200	4.00	2.40	722.43
52	75	1.588	95.83	50	5.00	1.80	234.17
53	75	1.588	95.83	100	5.00	1.80	454.06
54	75	1.588	95.83	200	5.00	1.80	836.92

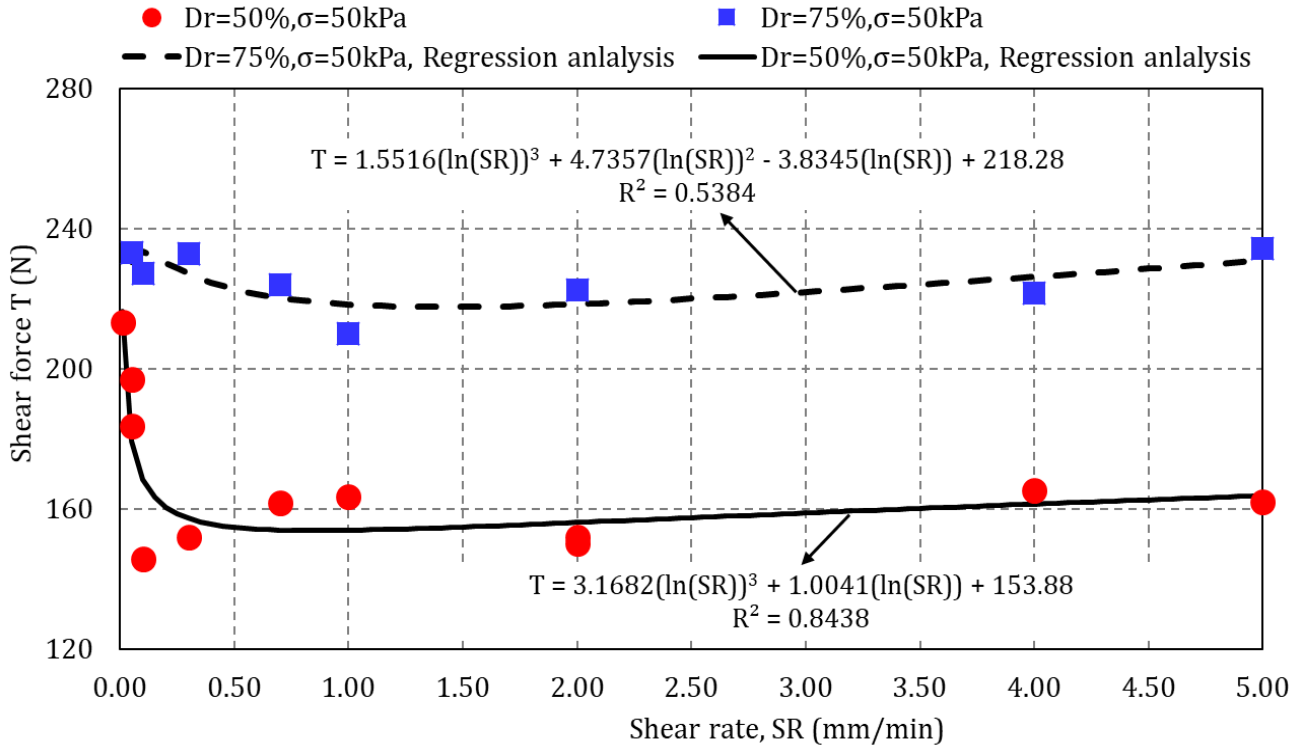

Fig. 9. Variations of shear force with increasing shear rates under σ=50kPa

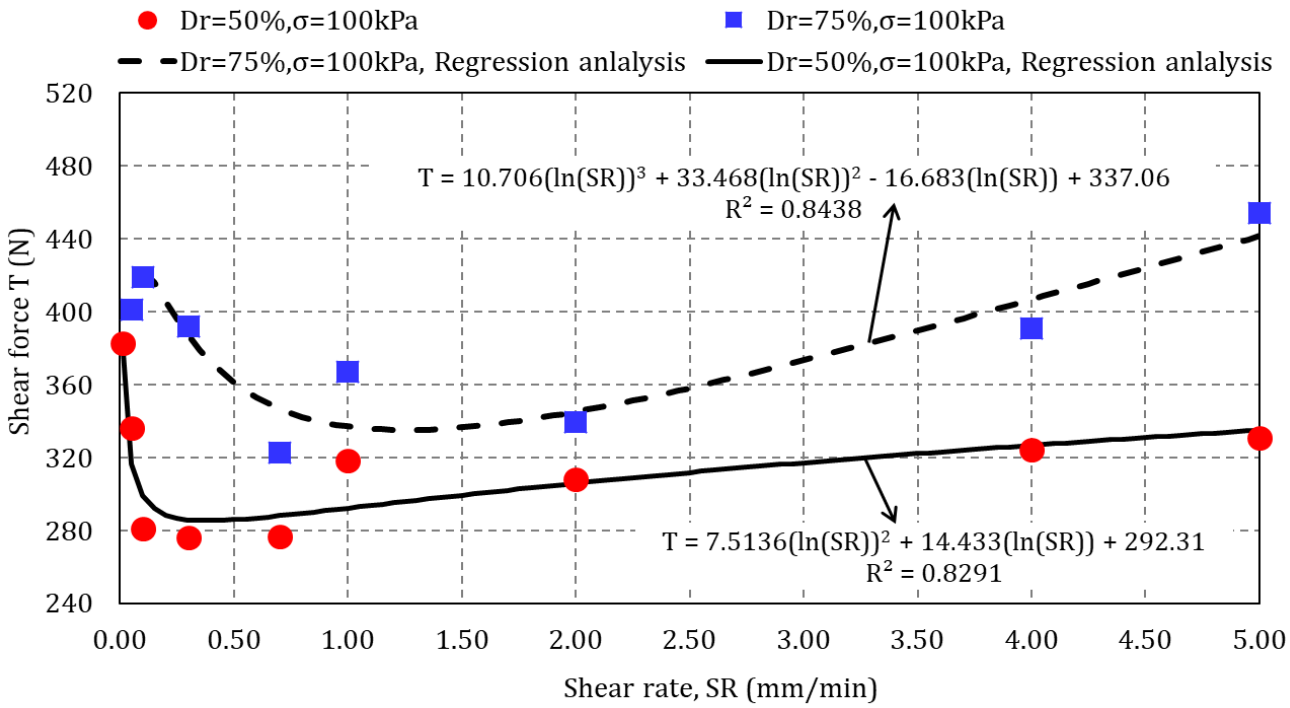

Fig. 10. Variations of shear force with increasing shear rates under σ=100kPa

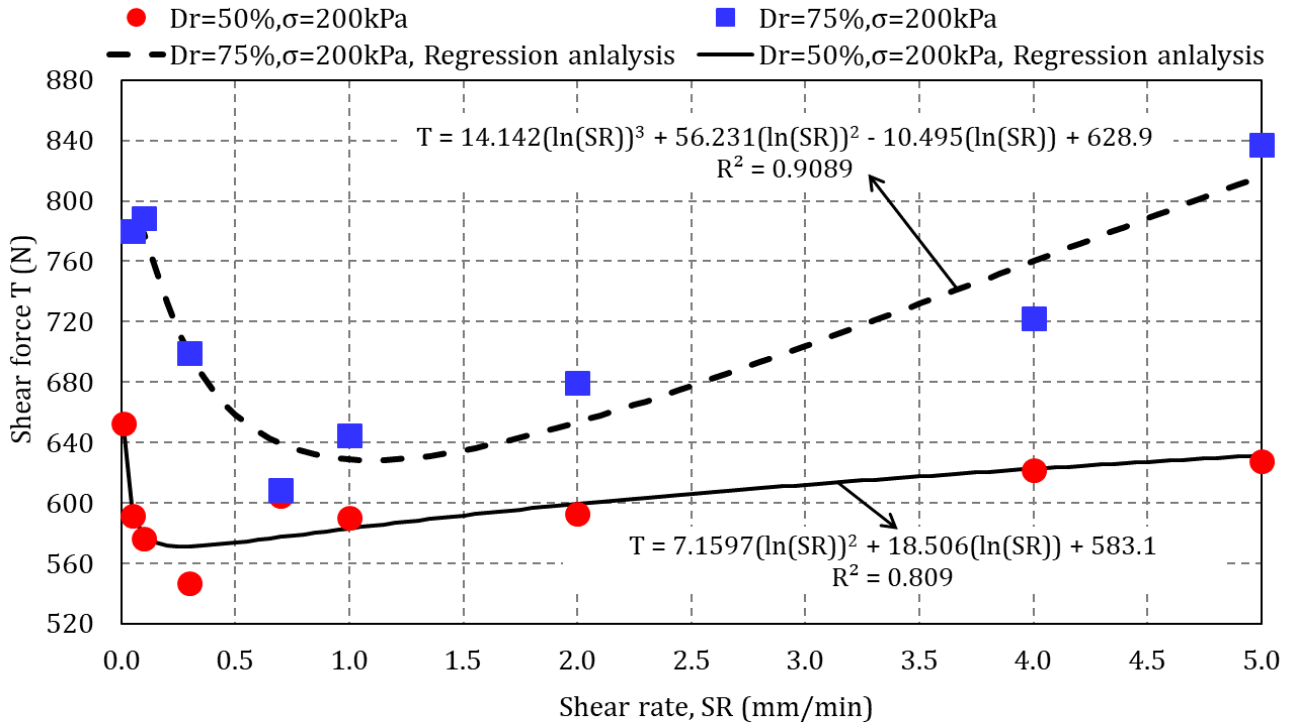

Fig. 11. Variations of shear force with increasing shear rates under σ=200kPa

The correlation function between shear force (T) and shear rate was determined using the least squares method. The findings revealed that for the dense coral sand, the correlation function took the form of a cubic equation with the variable ln(SR), while for the medium-dense coral sand, it adopted a quadratic equation. The appropriateness of these correlation functions was assessed through the R-squared value (R^2). The increase in normal stress corresponds to an increase in R^2. Moreover, in dense coral sand, R^2 ranged from 0.5384 to 0.9089, while in medium-dense coral sand, it varied from 0.7575 to 0.8291. This implies that denser samples or higher normal stress led to a

reduction in the dispersion of the test results. Consequently, the shear force correlation function, based on the shear rate as described above, demonstrated higher accuracy under denser sample conditions or increased normal stress.

Within the investigated shear rate range from 0.01 mm/min to 5 mm/min, a consistent trend was observed in the test results. For medium-dense coral sand, the largest measured peak shear force occurred at the lowest shear rate, whereas for dense coral sand, the largest measured peak shear force was associated with the highest shear rate. The percentage difference between the minimum and maximum measured peak shear forces, summarized in Table 3, ranges from 11.55% to 46.35% within the examined shear rate interval. Although each test condition was represented by a single experiment, the magnitude of these differences and their systematic variation with relative density suggest that shear rate exerts a non-negligible influence on the measured peak shear force under the tested conditions. Accordingly, these results highlight the importance of considering shear rate effects when interpreting direct shear test results on coral sand, while recognizing that additional repeat tests are required to quantitatively assess experimental scatter and further confirm the observed trends.

Table 3. The discrepancy in shear force values within the analyzed range of shear rates

Relative density, Dr (%)	Normal stress (kPa)	Peak shear force, T (N)		Percent deviation (%)
		min	max	
50	50	145.66	213.18	46.35
	100	276.38	382.64	38.45
	200	547.13	652.53	19.26
75	50	209.93	234.17	11.55
	100	322.48	454.06	40.80
	200	608.38	836.92	37.57

Next, based on the regression functions of the shear force depending on the shear rate $T_{\sigma_i}^{D_r} = f(SR)$ (as shown in Fig. 9 to Fig. 11), the shear strength parameters of coral sand corresponding to each relative density were determined according to the following formula being provided in the GOST 12248-2010 [32]:

$$\tan(\varphi_{D_r}) = \frac{3.\sum_{i=1}^{3}\frac{T_{\sigma_i}^{D_r}}{A}.\sigma_i - \sum_{i=1}^{3}\frac{T_{\sigma_i}^{D_r}}{A}.\sum_{i=1}^{3}\sigma_i}{3.\sum_{i=1}^{3}\sigma_i^2 - \left(\sum_{i=1}^{3}\sigma_i\right)^2} \quad (1)$$

$$C_{D_r} = \frac{\sum_{i=1}^{3}\frac{T_{\sigma_i}^{D_r}}{A}.\sum_{i=1}^{3}\sigma_i^2 - \sum_{i=1}^{3}\sigma_i.\sum_{i=1}^{3}(\frac{T_{\sigma_i}^{D_r}}{A}.\sigma_i)}{3.\sum_{i=1}^{3}\sigma_i^2 - \left(\sum_{i=1}^{3}\sigma_i\right)^2} \quad (2)$$

where:

φ_{D_r}, C_{D_r} - the internal friction angle and unit cohesion of the coral sand corresponding to the relative density

$A = \frac{\pi.D^2}{4}$ - area of the sample (D – diameter of sample, D=63.5mm)

$T_{\sigma_i}^{D_r}$ - The shear force corresponds to the relative density D_r and the normal stress acting on the coral sample σ_i

Substitute the regression functions of the shear force depending on the shear rate into Equations (1) and (2), the relationship between internal friction angle (or unit cohesion) and shear rate for different relative densities was established (Fig. 12 to Fig. 15). It becomes evident that the change in internal friction angle with shear rate is similar to that observed in shear force. It's seen that the internal friction angle reflects the trend of peak shear force over multiple values of shear rate with both the levels of compactness (D_r=50% and D_r=75%). Specifically, similar to the trend of the

influence of shear rates on peak shear forces that there is a distinct shear rate (SR_{so}) existing for the internal friction angle to reach its minimum value. However, there was a slight difference in behavior for the cohesion. The cohesion at relative density D_r=50% tends to gradually decrease, remaining relatively stable with increasing shear rate. For cohesion at relative density D_r=75%, a contrary trend to the internal friction angle is noted, with a shear rate (SR=0.5mm/min) identified for cohesion to reach its maximum value. After the maximum value, the cohesion of dense sand decreased significantly with increasing SR. The observed difference can be reasonably explained by the concept of apparent cohesion in coral sand, which has been widely reported in the literature for granular materials with angular and irregular particles. This apparent cohesion arises from mechanical interlocking between particles, and is commonly reflected by a non-zero intercept when fitting a Mohr-Coulomb failure envelope. With increasing shear rate, the mobilization and degradation of interlocking contacts are expected to evolve, which can influence the apparent cohesion parameter obtained from macroscopic shear tests. Specimens with higher relative density are characterized by a greater number and stronger interlocking contacts compared to looser specimens. Accordingly, for specimens at D_r = 50%, where fewer interlocking contacts are mobilized, the apparent cohesion shows only a limited sensitivity to changes in shear rate. In contrast, for specimens at D_r = 75%, where interlocking effects are more pronounced, the apparent cohesion exhibits a more evident reduction as shear rate increases. This trend is consistent with the mechanical interpretation of particle interlocking in dense granular assemblies and with observations reported in previous studies on coral sand.

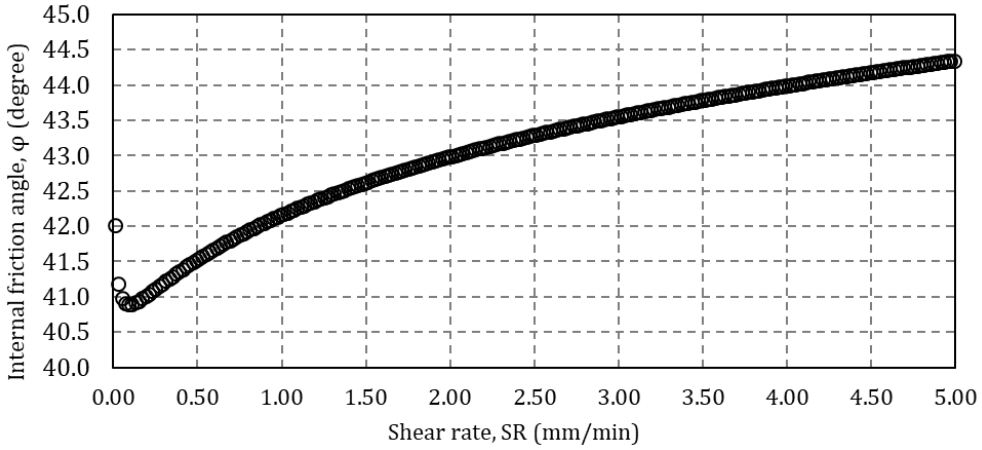

Fig. 12. Relationship between SR and φ for medium-dense coral sand

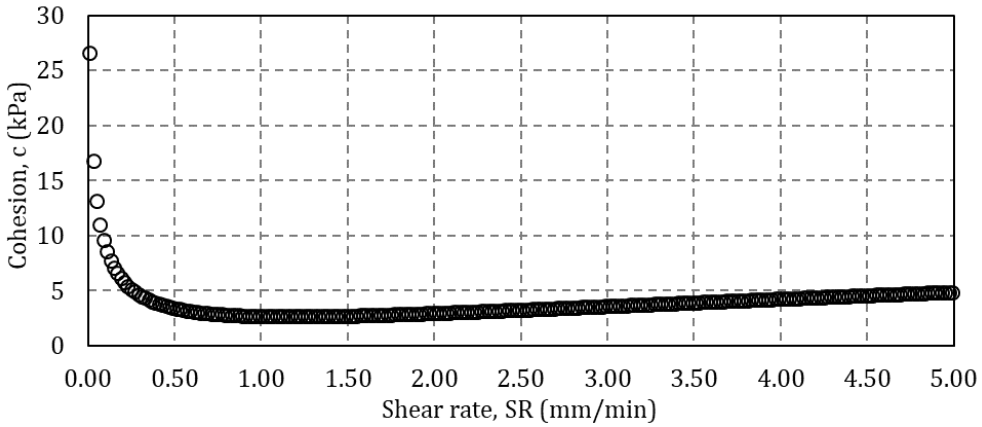

Fig. 13. Relationship between SR and cohesion for medium-dense coral sand

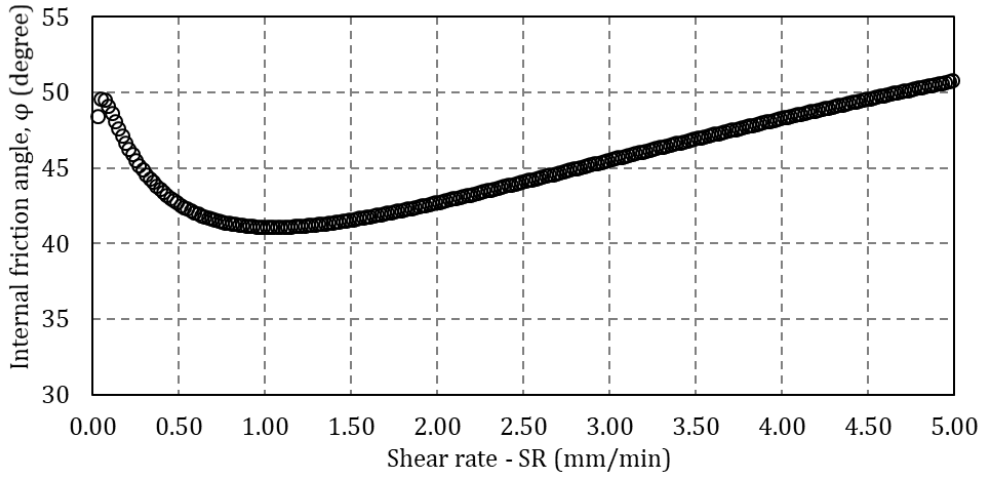

Fig. 14. Relationship between SR and φ for dense coral sand

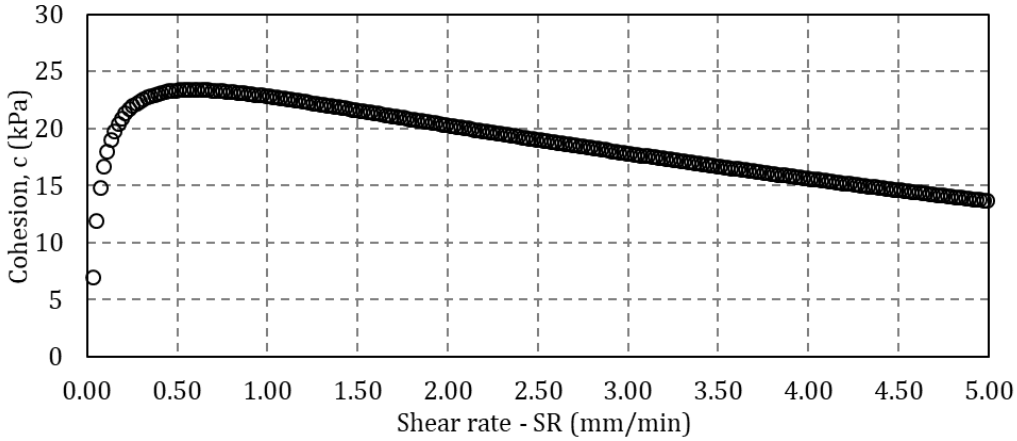

Fig. 15. Relationship between SR and cohesion for dense coral sand

Compared with the influence of shear rate on the shear strength parameters of common sands, the behavior of coral sand is considerably more complex due to its distinctive particle morphology, high intraparticle porosity, and crushability. Beren et al. [33] investigated the effect of shear rate on the strength characteristics of various soils with different particle size distributions under both wet and dry conditions. Their results indicated that, in all cases, the internal friction angle increased whereas the apparent cohesion decreased with increasing shear rate, and the shear strength followed a Mohr–Coulomb failure envelope. Although a relatively wide range of shear rates was applied, the overall variation in shear strength parameters was limited, generally less than 10%. Similar trends have been reported for silica sand and clean sands under undrained conditions [34], as well as for mixed sands at optimum moisture content [35].

In contrast, coral sand exhibits pronounced shear-rate sensitivity without a monotonic trend. Depending on the applied shear rate range, the internal friction angle may either increase or decrease, with a corresponding inverse variation in apparent cohesion. This non-uniform rate dependency suggests that constitutive models developed for conventional quartz-based sands may not adequately capture the complex mechanical response of coral sand under varying shear rates.

4.2. Effect of Repeated Loading on the Shear Behavior of Coral Sand

Fig. 16 to Fig. 19 illustrate the correlation between shear force (T) and horizontal displacement (U) obtained from 24 tests across various amplitudes of cyclic loads, shear rates, and normal stresses, considering different relative

densities of the coral sand samples.

For the medium-dense specimens, Figs. 16 and 17 indicate that in the absence of cyclic loading (N = 0), the shear stress-displacement (T–U) relationship did not exhibit a pronounced peak; the maximum shear force was only marginally higher than the residual value. In contrast, once cyclic loading was applied, all cases (N > 0) displayed a distinct peak in the T-U curves. A sharp increase in peak shear force was observed even at a low number of load cycles (N = 10 and 20). However, no clear monotonic relationship could be identified between the number of cycles and the magnitude of peak strength increment. Following peak mobilization, specimens subjected to cyclic loading exhibited strain-softening behavior, with shear stress decreasing toward a critical state and eventually reaching a residual strength slightly higher than that of the N = 0 case. Strain softening is typically associated with dense sand or low normal stress conditions. Given that the applied normal stress was 100 kPa, the observed softening in the medium-dense specimens after cyclic loading can reasonably be attributed to densification induced during cyclic loading. The rapid increase in density at relatively low cycle numbers (N = 10 and 20) suggests a complex rearrangement mechanism, likely governed by the highly angular, crushable, and intraporous nature of coral sand particles. Particle interlocking enhancement, local crushing, and pore collapse may collectively contribute to the rapid gain in peak strength.

For the dense coral sand, as shown in Figs. 18 and 19, the dense specimens exhibited a clear peak shear force even without cyclic loading (N = 0), and the peak strength was significantly higher than the residual strength. After cyclic loading, only a slight increase in peak shear force was observed. Post-peak softening occurred in all cases, and the residual strengths converged to nearly identical values, comparable to that of the non-cyclic condition. This behavior suggests that for initially dense coral sand, cyclic loading produces limited additional densification, as the soil fabric is already in a highly compact state. Consequently, while peak strength is marginally enhanced, the critical-state and residual strengths remain essentially unaffected, indicating that shear resistance of dense coral sand is primarily governed by the intrinsic frictional characteristics and is less volatile than that of medium-dense sand. To clearly see the different behaviors between medium-dense sand and dense sand, Fig. 20 and Fig. 21 show the percentage change in shear force relative to the number of cycles for medium-dense coral sand and dense coral, respectively. The largest increase in peak shear force for medium-dense coral sand was 55%, whereas for dense coral sand, the maximum increase in peak shear force was 21%. Thus, it is confirmed that, under cyclic loading conditions, the medium-dense coral sand experiences a more significant increase in peak shear force, compared to the dense coral sand. This difference is related to the initial compactness level of the samples. The initial compactness level of dense coral sand is higher than that of the medium-dense coral sand, therefore, when the cyclic load was not applied (N=0), the dense coral sand exhibited significantly higher peak shear forces (about 360N, Figs. 18 and 19) than the medium-dense coral sand (about 270N, Figs. 16 and 17). However, during the cyclic loadings, the medium-dense coral sand samples could increase their compactness more significantly than the dense sand samples could. As a result, peak shear forces for the medium-dense sand samples increase more significantly after cyclic loadings (36-55%, Fig. 20), in comparison to corresponding peak shear forces of the dense sand samples (13-21%, Fig. 21). A finite-difference assessment of the experimental measurements indicates a rapid increase in the percentage gain of peak shear force during the first 10 cycles (about 4÷5% per cycle). After approximately 20 cycles, the curve becomes more plateau-like, with a much smaller slope (typically

within about ±0.5% per cycle for A = 0.8 mm and close to 0% per cycle for A = 1.6 mm over 30÷40 cycles), indicating a more stabilized increase level rather than a continuing monotonic growth.

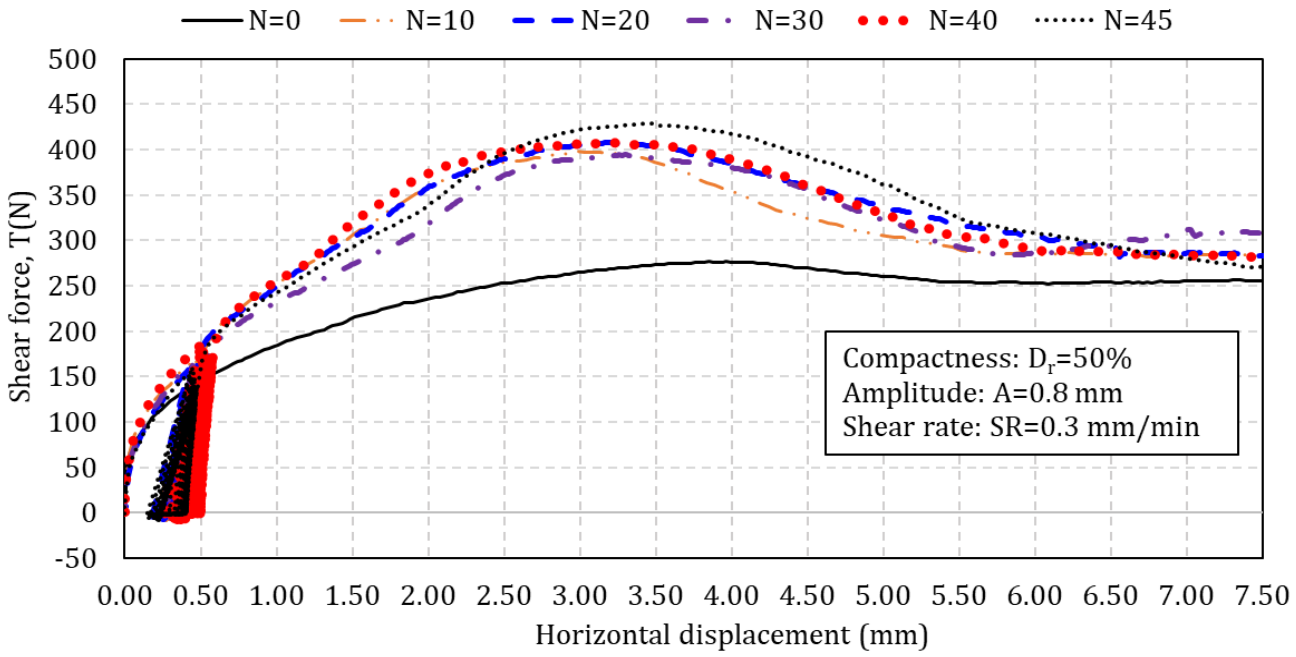

Fig.16. Shear Force-Displacement Relationship: Amplitude (A) = 0.8mm, Shear Rate (SR) = 0.3mm/min, and Vertical Load (σ) = 100kPa for medium-dense coral sand

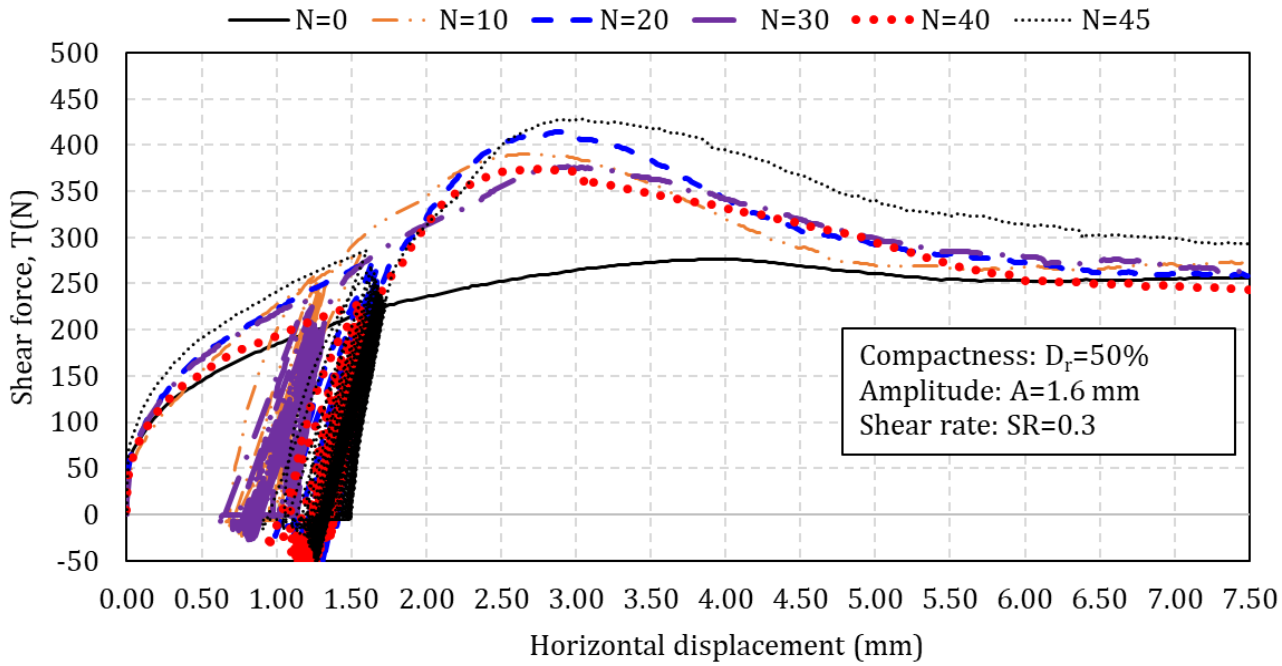

Fig. 17. Shear Force-Displacement Relationship: Amplitude (A) = 1.6 mm, Shear Rate (SR) = 0.3mm/min, and Vertical Load (σ) = 100kPa for medium-dense coral sand

In summary, the mechanical response of coral sand under cyclic loading suggests that the observed increase in peak shear force is primarily attributable to densification induced during cyclic loading. For the case without cyclic loading (N = 0), the medium-dense and dense specimens exhibited markedly different behaviors, particularly in terms of peak and post-peak responses. However, after the application of cyclic loading, this difference became significantly reduced. Notably, the peak shear forces of the medium-dense specimens approached approximately 400 N, which is

comparable to the peak shear forces measured for the dense specimens. A similar convergence was observed for the residual shear forces, with medium-dense sand reaching values of approximately 280 N, nearly identical to those of the dense sand. These results indicate that cyclic loading effectively modifies the soil fabric and packing state of medium-dense coral sand, leading to a mechanical response comparable to that of initially dense sand. This convergence in both peak and residual strengths highlights the strong influence of cyclic-induced densification on the shear behavior of coral sand.

4. Conclusions

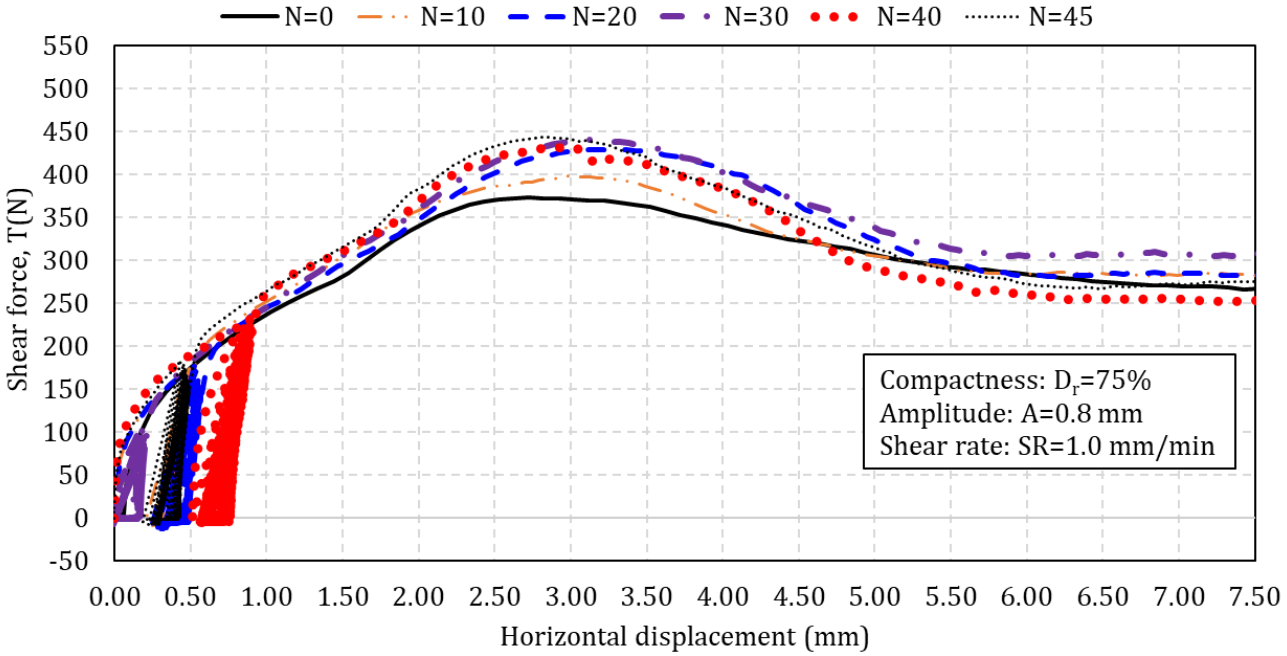

Fig. 18. Shear Force-Displacement Relationship: Amplitude (A) = 0.8 mm, Shear Rate (SR) = 1mm/min, and Vertical Load (σ) = 100kPa for dense coral sand

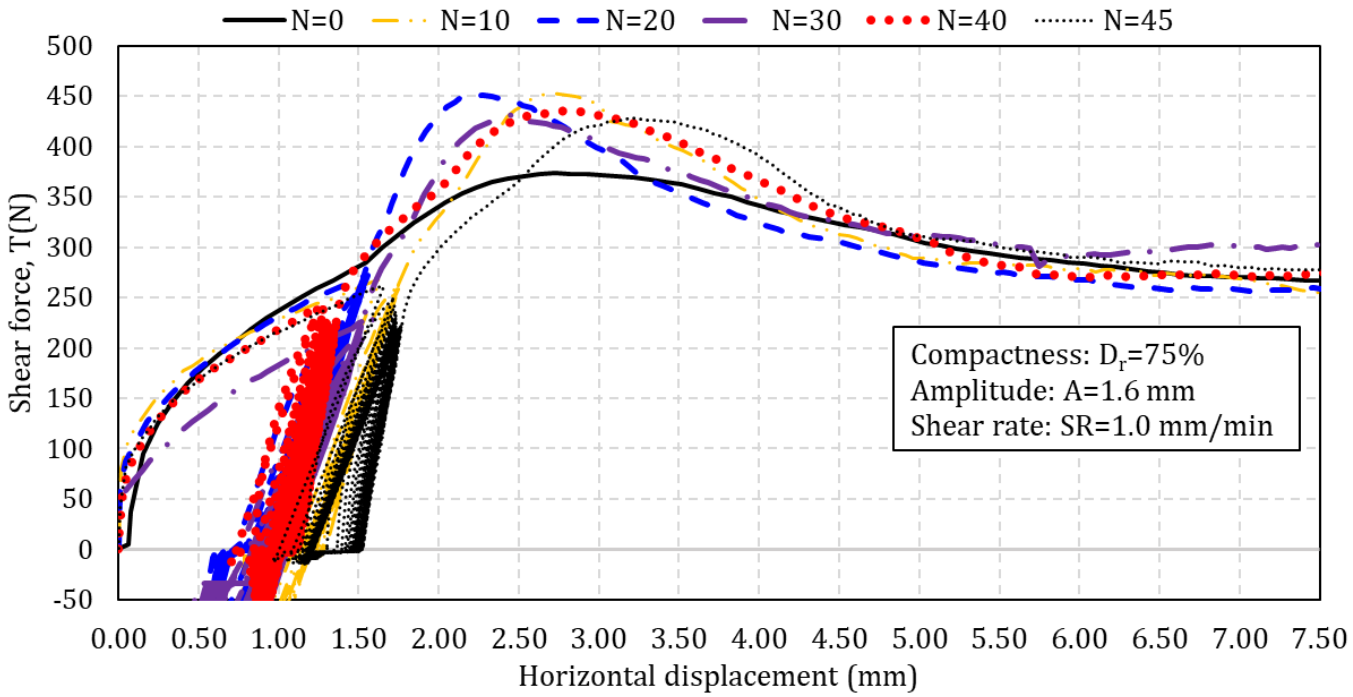

Fig. 19. Shear Force-Displacement Relationship: Amplitude (A) = 1.6 mm, Shear Rate (SR) = 1.00 mm/min, and Vertical Load (σ) = 100kPa for dense coral sand

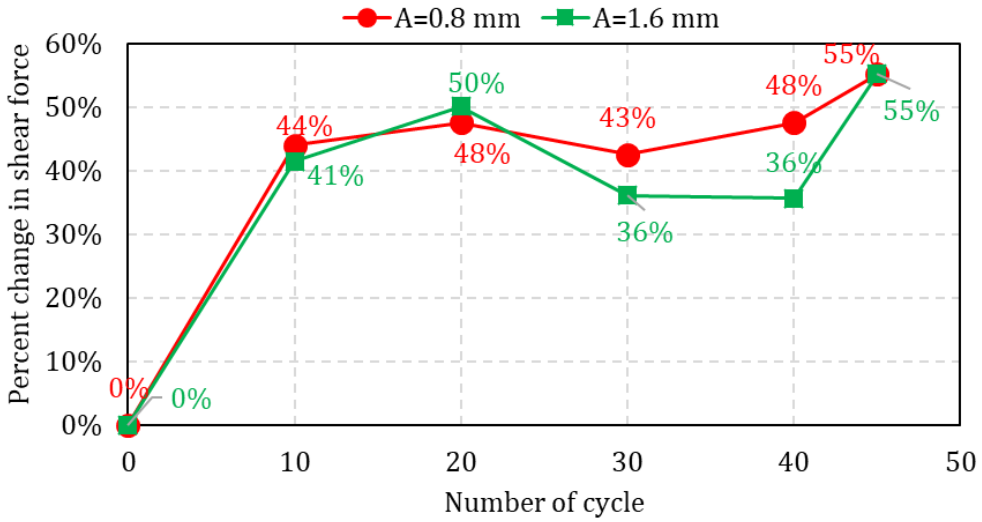

Fig. 20. Percentage change in shear force relative to the number of cycles for medium-dense coral sand

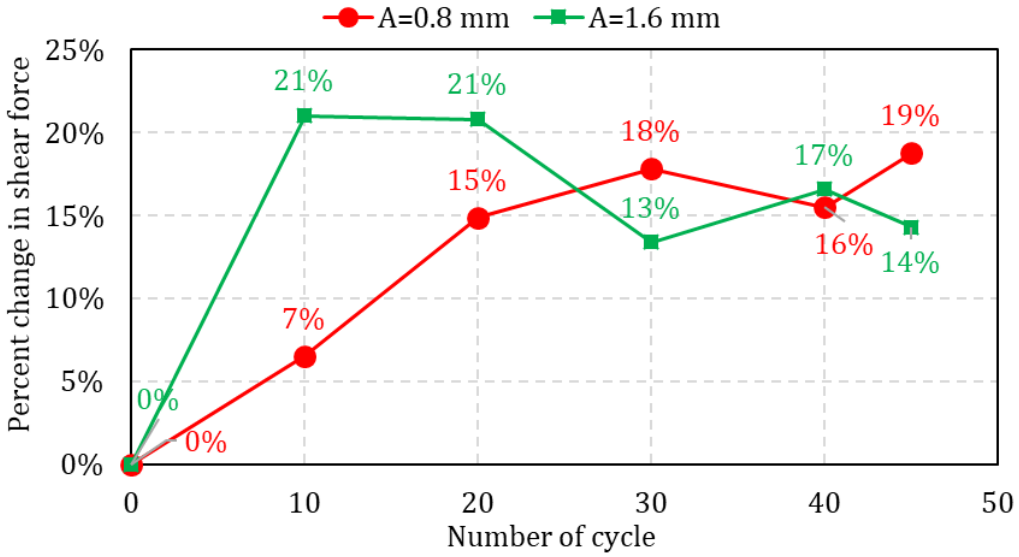

Fig. 21. Percentage change in shear force relative to the number of cycles for dense coral sand

In this paper, seventy-four direct shear tests and cyclic shear tests were conducted to investigate the shear strength characteristics of a coral sand subjected to different shear rates and cyclic loads. The main findings are as follows:

For the sand in this study, there exists a specific shear rate (SR_{so}) at which the shear force reaches its minimum value, representing the lowest shear strength. For the medium-dense state, SR_{so} was approximately 0.3mm/min, while for the dense state, SR_{so} was around 1.0mm/min. The variation between the minimum and maximum shear force values between the examined shear rate range ranged from 11.55% to 46.35%. This highlights the noticeable influence of shear rate on the shear strength of the coral sand.

For dense coral sand, the correlation function between shear force (T) and shear rate (SR) takes the form of a cubic equation with the variable ln(SR), while for medium-dense coral sand, the correlation function is a quadratic equation. The variation in internal friction angle with shear rates reflects the variation of shear force. However, the cohesion behavior is slightly different. The cohesion at relative density Dr=50% tended to gradually decrease with increasing SR first, thereafter remaining relatively stable with increasing SR. Conversely, for the cohesion at relative density D_r=75%, a contrary trend was observed, with a shear rate (SR=0.5mm/min)

identified for the cohesion to reach its maximum value.

Cyclic loading has a significant influence on the shear characteristics of the medium-dense coral sand. After cyclic loading, the peak shear force demonstrates a sharp increase, even a low number of load cycles was applied. For the dense sand, a noticable rise after cyclic loading in peak shear force was observed when the number of cycles was below 20. Beyond 20 cycles, the peak shear force could increase or decrease, but not noticeably. Medium-dense coral sand experiences a much greater increase in peak shear force, compared to dense coral sand, this phenomenon can be explained that the medium-dense sand is able to increase its compactness more significantly than dense coral sand during cyclic loadings. The largest increase in peak shear force for medium-dense coral sand was 55%, whereas for dense coral sand, the maximum increase in peak shear force was 21%.

In general, shear rate, cyclic load, relative density, and normal stress have clear influences on shear strength behavior of coral sand. It is important to understand these characteristics well when designing an offshore structure on coral sand ground or using coral sand for construction purposes.

Limitations and Future Work

The main limitations of the present study can be summarized as follows.

- For each testing condition, only a single test was conducted, which prevents a rigorous statistical evaluation of experimental variability, despite the use of a fully automated testing system.

- The cyclic shear tests were performed under low-rate, quasi-static, displacement-controlled conditions and therefore do not represent dynamic loading, cyclic strength, or liquefaction behavior.

- Changes in void ratio and specimen height during cyclic loading were not measured; consequently, the interpretation of post-cyclic strength increase as a densification effect remains a plausible hypothesis rather than a verified mechanism.

- The range of testing parameters, including normal stress, shear rate, displacement amplitude, and number of cycles, was relatively limited.

Based on these limitations, future research should focus on conducting replicate tests for statistical assessment, extending cyclic tests to stress-controlled and higher-rate loading conditions, incorporating direct measurements of volumetric response during cyclic shearing, and exploring a broader range of loading and environmental conditions to improve the generality of the conclusions.

Declarations of Conflict of Interest

The authors declare that they have no conflict of interest.

References

[1] R.A. Arumugam and K Ramamurthy. (1996). Study of compressive strength characteristics of coral aggregate concrete. *Magazine of Concrete Research*, 48(176), 141-148. https://doi.org/10.1680/macr.1996.48.176.141

[2] Y. Amini, A. Hamidi, and E. Asghari. (2014). Shear strength–dilation characteristics of cemented sand–gravel mixtures. *International Journal of Geotechnical Engineering*, 8(4), 406-413. https://doi.org/10.1179/1939787913Y.0000000026

[3] F.A.M. Marinho, O.M. Oliveira, H. Adem, and S. Vanapalli. (2013). Shear strength behavior of compacted unsaturated residual soil. *International Journal of Geotechnical Engineering*, 7(1), 1-9. https://doi.org/10.1179/1938636212Z.00000000011

[4] S. MotahariTabari, and I. Shooshpasha. (2018). Evaluation of coarse-grained mechanical properties using small direct shear test. *International Journal of Geotechnical Engineering*, 15(6), 667-679.

https://doi.org/10.1080/19386362.2018.1505310

[5] A.F. Ikechukwu, M.M. Hassan, and A. Moubarak. (2021). Swelling stress effects on shear strength resistance of subgrades. *International Journal of Geotechnical Engineering*, 15(8), 939-949. https://doi.org/10.1080/19386362.2019.1656445

[6] Y. Mahmoudi, A.C. Taiba, M. Belkhatir, A. Arab, and T. Schanz. (2018). Laboratory study on undrained shear behaviour of overconsolidated sand–silt mixtures: effect of the fines content and stress state. *International Journal of Geotechnical Engineering*, 12(2), 118-132. https://doi.org/10.1080/19386362.2016.1252140

[7] S. Rouhanifar, M. Afrazi, A. Fakhimi, and M. Yazdani. (2021). Strength and deformation behaviour of sand-rubber mixture. *International Journal of Geotechnical Engineering*, 15(9), 1078-1092. https://doi.org/10.1080/19386362.2020.1812193

[8] W. Zhe, D. Zhigang, L. Shouding, W. Jianping, MA. Bin, L. Xiao, Z. Zhongming, and L. Zhiqing. (2020). Shear mechanical properties of dredged coral sands from south China sea, China. *Journal of Engineering Geology*, 28(1), 77-84.

[9] W. Wang, W. Li, and Z. Yao. (2019). Experimental study on shear characteristics of reef coral sand. *IOP Conference Series: Earth and Environmental Science,* 358(5), 052042. DOI 10.1088/1755-1315/358/5/052042

[10] Y. Zhang, R. Zhang, C. Yu, H. Luo, and Z. Deng. (2023). Study on shear characteristics of calcareous sand with different particle size distribution. *Frontiers in Earth Science*, 11, 1163930. https://doi.org/10.3389/feart.2023.1163930

[11] M. Beren, I. Çobanoglu, S.B. Çelik, and Ö. Ündül. (2020). Shear rate effect on strength characteristics of sandy soils. *Soil Mechanics and Foundation Engineering*, 57, 281-287. https://doi.org/10.1007/s11204-020-09667-y

[12] J.A. Yamamuro, A.E. Abrantes, and P.V. Lade. (2011). Effect of strain rate on the stress-strain behavior of sand. *Journal of Geotechnical and Geoenvironmental Engineering*, 137(12), 1169-1178. https://doi.org/10.1061/(ASCE)GT.1943-5606.0000542

[13] K. Sweta and S.K.K. Hussaini. (2018). Effect of shearing rate on the behavior of geogrid-reinforced railroad ballast under direct shear conditions. *Geotextiles and Geomembranes*, 46(3), 251-256. https://doi.org/10.1016/j.geotexmem.2017.12.001

[14] M.L. Silver, F. Tatsuoka, A. Phukunhaphan, and A.S. Avramidis. (1980). Cyclic undrained strength of sand by triaxial test and simple shear test. *Proceedings of the 7th world conference on earthquake engineering, pp. 281-288.*

[15] A. Erken and B.M. Can Ulker. (2007). Effect of cyclic loading on monotonic shear strength of fine-grained soils. *Engineering Geology*, 89(3-4), 243-257. https://doi.org/10.1016/j.enggeo.2006.10.008

[16] N.-P. Doan, S.-S. Park, and D.-E. Lee. (2020). Assessment of Pohang earthquake-induced liquefaction at Youngil-man port using the UBCSAND2 model. *Applied Sciences*, 10(16), 5424. https://doi.org/10.3390/app10165424

[17] P. Ray and R.B. Sahu. (2021). A parametric study on cyclic strength of coastal sand of Digha in West Bengal, India. *International Journal of Geo-Engineering*, 12, 5. https://doi.org/10.1186/s40703-020-00134-z

[18] Z. Ding, S.-H. He, Y. Sun, T.-D. Xia, and Q.-F. Zhang. (2021). Comparative study on cyclic behavior of marine calcareous sand and terrigenous siliceous sand for transportation

infrastructure applications. *Construction and Building Materials*, 283, 122740. https://doi.org/10.1016/j.conbuildmat.2021.122740

[19] S.-H. He, Z. Ding, T.-D. Xia, W.-H. Zhou, X.-L. Gan, Y.-Z. Chen, and F. Xia. (2020). Long-term behaviour and degradation of calcareous sand under cyclic loading. *Engineering Geology*, 276, 105756. https://doi.org/10.1016/j.enggeo.2020.105756

[20] G. Wang and J. Zha. (2020). Particle breakage evolution during cyclic triaxial shearing of a carbonate sand. *Soil Dynamics and Earthquake Engineering*, 138, 106326. https://doi.org/10.1016/j.soildyn.2020.106326

[21] W. Ma, Y. Qin, Q. Wu, G. Zhang, and G. Chen. (2023). Cyclic failure mechanisms of saturated marine coral sand under various consolidations. *Applied Ocean Research*, 131, 103450. https://doi.org/10.1016/j.apor.2022.103450

[22] Q. You, W. Ma, S. Wu, Q. Wu, Z. Lei, and G. Chen. (2023). Fixed-axis shear characteristics of marine coral sand under various consolidation conditions. *Ocean Engineering*, 286, 115642. https://doi.org/10.1016/j.oceaneng.2023.115642

[23] N.S. Hung, H. Anh. (2020). Experimental study on the bearing capacity of weak soil with filling sand layer above using D-BOX soil bags (in Vietnamese). *Journal of Materials & Construction*, 2020(3), 85-89.

[24] ASTM International. (2011). Designation: D2487-11 standard practice for classification of soils for engineering purposes (unified soil classification system).

[25] D.W. Taylor. (1948). Fundamentals of soil mechanics. *Soil Science*, 66(2), 161.

[26] A.W. Skempton and A.W. Bishop. (1950). The measurement of the shear strength of soils. *Géotechnique*, 2(2), 90-108. https://doi.org/10.1680/geot.1950.2.2.90

[27] ASTM International. (2012). ASTM Standard. D3080/D3080M—11 Direct Shear Test of Soils Under Consolidated Drained Conditions.

[28] S. Shibuya, T. Mitachi, and S. Tamate. (1997). Interpretation of direct shear box testing of sands as quasi-simple shear. *Géotechnique*, 47(4), 769-790. https://doi.org/10.1680/geot.1997.47.4.769

[29] M.L. Lings and M.S. Dietz. (2004). An improved direct shear apparatus for sand. Géotechnique, 54(4), 245-256. https://doi.org/10.1680/geot.2004.54.4.245

[30] M. Dolz, A. Casanovas, J. Delegido, and M.J. Hernández. (2004). An experimental setup to verify stokes law using an electronic balance. *Revista Mexicana de Física*, 50(1), 29-32.

[31] M.Y. Fattah and F.A. Salman. (2006). The active zone for heave of expansive soils. *Proceedings of the 4th Jordanian Civil Engineering Conference*.

[32] Russian National Standard. (2011). GOST 12248-2010. Soils - Methods for laboratory determination of strength and deformability characteristics.

[33] M. Beren, I. Çobanoglu, S.B. Çelik, Ö. Ündül. (2020). Shear rate effect on strength characteristics of sandy soils. *Soil Mechanics and Foundation Engineering*, 57, 281-287. https://doi.org/10.1007/s11204-020-09667-y

[34] J.A. Yamamuro and P.V. Lade. (1993). Effects of strain rate on instability of granular soils. *Geotechnical Testing Journal*, 16(3), 304–313. https://doi.org/10.1520/GTJ10051J

[35] A. Chegenizadeh, M. Keramatikerman, H. Nikraz. (2020). Effect of Shear Rate Shear Strength of Sand Mixed with Fibre-Pine Shaving. *International Journal of Emerging Trends in Engineering Research*, 8(4), 1284-1288. https://doi.org/10.30534/ijeter/2020/56842020